JSEE Vol. 21, No. 1, 2019 DOI:10.48303/jsee.2019.240804

Probabilistic Fault Displacement Hazard Analysis of Choman Dam Site, West of Iran

Naser Hafezi Moghaddas[1] and Chin Leo[2]*

1. Professor of Engineering Geology, Ferdowsi University of Mashhad, Iran,
* Corresponding Author; email: nhafezi@um.ac.ir
2. Professor of Geotechnical Engineering, School of Computing, Engineering and Math, Western Sydney University, Australia

Received: 23/05/2018
Accepted: 16/02/2019

ABSTRACT

In this paper, the surface fault displacement hazard at the Choman dam is evaluated by a new approach of probability fault displacement hazard analysis (PFDHA). For this, fault map and fault characteristics of area are determined based on the aerial photographs, satellite image, and field studies. In this study, Piranshahr fault is divided into two segments of Piranshahr-Sardasht and Sardasht-Penjwen from across point of Armardeh fault. The empirical relationships proposed for strike-slip fault is applied to estimation of probability fault displacement hazard curve of Choman dam. The return periods of 10000 and 35000 years are selected for estimation of fault displacement for different earthquake design levels. Finally, fault displacement for Design Basic Earthquake (DBE), Maximum Design Earthquake (MDE) and Safety Evaluation Earthquake (SEE), 20, 30 and 65 cm are proposed.

Keywords:
Probabilistic fault displacement; Choman dam; Piranshhar Fault

1. Introduction

Surface faulting was responsible for damaging of some dams and their accessory structures during recent earthquakes [1-5]. Allen and Cluff [6] stated that the lack of appropriate criteria for recognition of active faults and evaluation of fault displacement were the main reasons for dam vulnerability in the past. The primary safety consideration for dam site selection is avoiding of active and potentially active faults [7]. However, in a seismic active tectonic area, such as Zagros zone in west of Iran, due to the current compressive stress, the majority of the gorges created by faults, all faults are suspected to be active; and therefore, some dam sites are inevitably were placed near the active faults. Hence, accurate evaluation of fault displacement is necessary for safety design of dam and its related structures [8-11].

The current state-of-practice (e.g., [12]) tends to estimate the fault displacement deterministically from empirical surface rupture vs. magnitude relationships, which commonly gives a conservative estimate of fault displacement especially for projects far from the main fault. The probabilistic fault displacement hazard assessment was firstly applied for a nuclear power plant in Nevada, USA [13]. The approach was followed, and its basic theory and empirical relationships were developed by other researchers [14-17]. In this study, the method proposed by Petersen et al. [14] for strike-slip faults were used to evaluate the probability fault displacement of Choman dam site in West of Iran (Figure 1).

2. Surface Faulting

Parameters of earthquake magnitude, depth of seismogenic layers, characteristics of material around

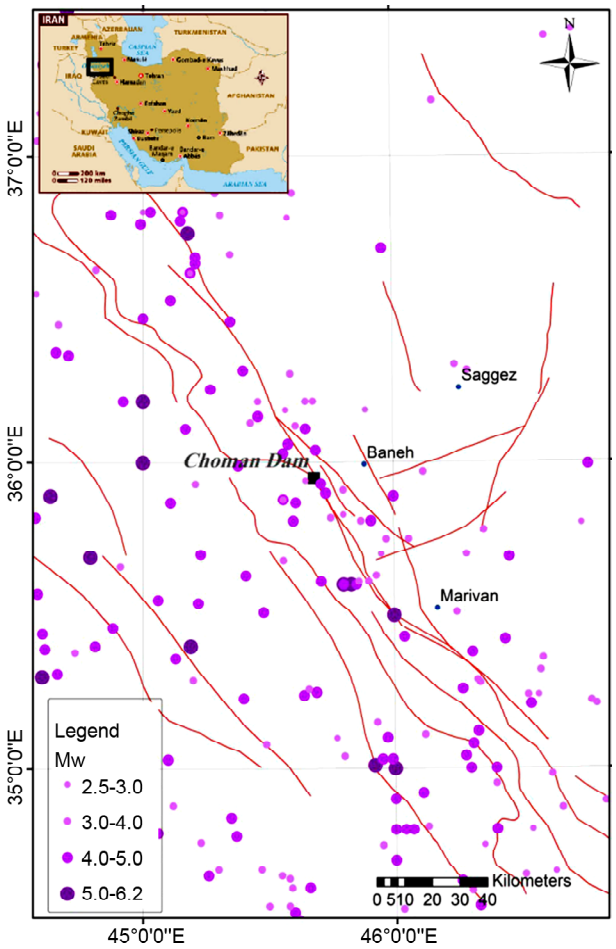

Figure 1. Location map of dam site under study.

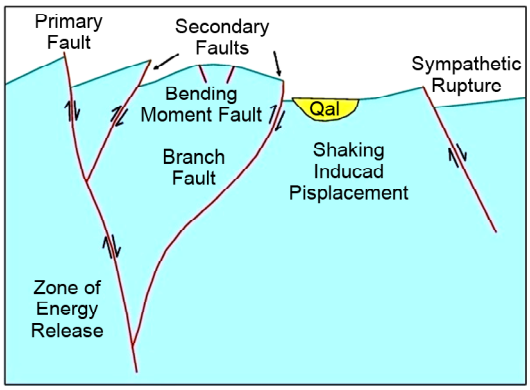

Figure 2. Different types of surface faulting [22].

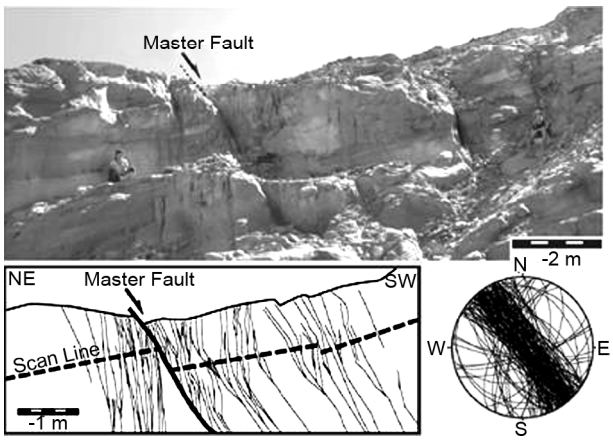

Figure 3. Faulting zone in the Wadi Arab normal fault, the displacement in the main fault was about 80 cm, but the total displacement reached up to 3.2 meters, and the width of fault zone in hanging wall block was greater than footwall [23].

the fault and geometry of the fault are effective parameters in surface faulting [18]. Although the faulting pattern is complex, it can be mainly divided into three parts: primary, secondary and induced or sympathetic form (Figure 2). The primary faulting occurred along the main fault and usually includes of the highest displacement. Secondary faulting is related to the minor faults that may exist several tens of meters away from the main fault [19]. Finally, sympathetic fault is an individual fault around the earthquake fault, which can be active simultaneously or a short time after the main shock. In a particular case, the sum of secondary fault displacements might be greater than the main fault displacement (Figure 3). The fault zone width increases from strike-slip to normal, reverse and thrust fault types [20]. Faulting pattern in soft material and minor displacement are complex and distributed, but it changes to the linear mode by increasing the strength of earth material and fault displacement [21]. Besides, the fault zone is usually wide spreaded in the fault bends.

3. Study Area

The earth fill dam of Choman, with a height of 100 meters, will be constructed on the Choman River, 30 km west of Baneh city, west of Iran (Figure 1). The dam site is located in the seismically active belt of folded Zagros and close to the Main Recent Zagros Fault (MRF) [24-25]. The MRF, with total length of 1350 km, is one of the great active faults in west of Iran, which the evidences of its recent activities and right-lateral motion are well-documented [26-27]. The new GPS network data indicates that the rate of displacement in MRF is about ~2-3 mm/y [28-29], while the past research proposed a higher rate of 10-17 mm/y [30]. The MRF has been divided into a few segments and the site under study is situated at the distance of 1.2 km from the Piranshahr segment on the northwest side of the MRF [31-32]. As with another part of MRF, Piranshahr fault has a NW-SE trend

and is mainly located on the border of Iran-Iraq, which received little attention in respect of other segments, due to security problems in the past decades. Mohajjel and Rasoli [33] stated that the Piranshahr fault in the south of Piranshahr city comprises of two right-lateral strike slip fault systems close to each other's, but with different normal and reverse components (Figure 4).

The recent earthquakes of 25/10/1970 Ms 5.3, 07/23/1981 Ms 5.6, 15/01/1995 Ms 4.9, 1/09/2000 Mw 4.4, 19/12/2002 Mw 4.8 and 06/06/2006 Mw 4.8 (Figure 1), with a normal right lateral strike-slip motion, has been attributed to the activity of this fault [33-34]. Berberian [35] and Talebian and Jackson [27] reported different trends for Piranshahr fault from south of Baneh city toward the southeast. Based on the Talebian and Jackson [27], the length of fault is more than 150 km (Figure 5). The Piranshahr fault mainly passes through the Zab River (Figure 5), and the right lateral displacement of the fault is clearly visible in the aerial photograph and satellite images (Figure 6).

In this study, Piranshahr fault is divided into two segments of Piranshahr-Sardasht and Sardasht-Penjwen from across point of Armardeh fault. The general trend of the two segments is the same, but the Piranshahr-Sardasht segment about 5 km offsetted to the east and has a more rugged

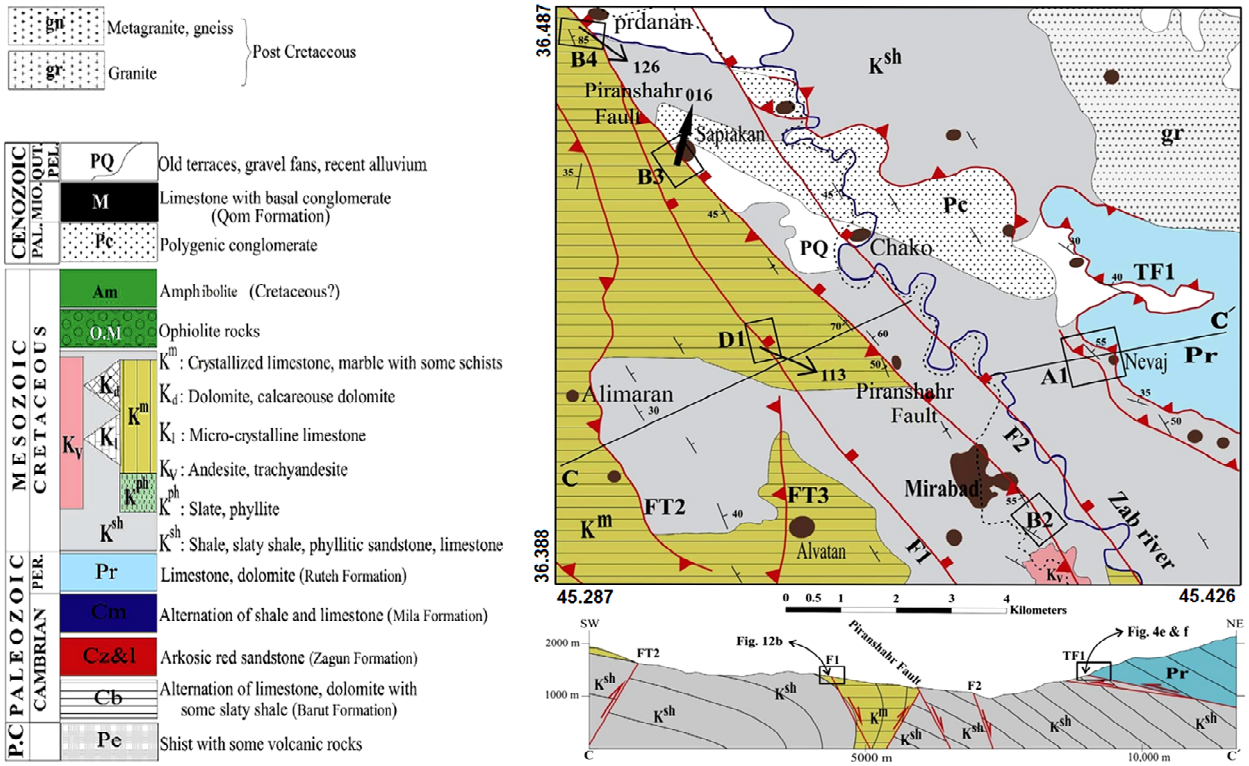

Figure 4. Different fault systems in Piranshahr Fault Zone in the south of Piranshahr city [33].

Figure 5. Following of Zab River from Piranshahr fault trend (Piranshahr -Sardasht).

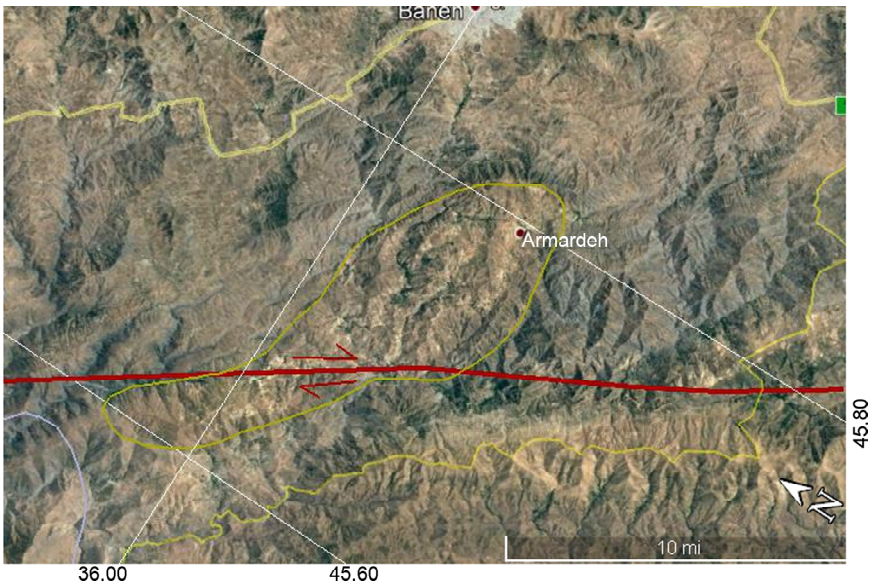

Figure 6. About 3 km right-lateral displacement of Baneh Batholith mass along the Piranshahr fault.

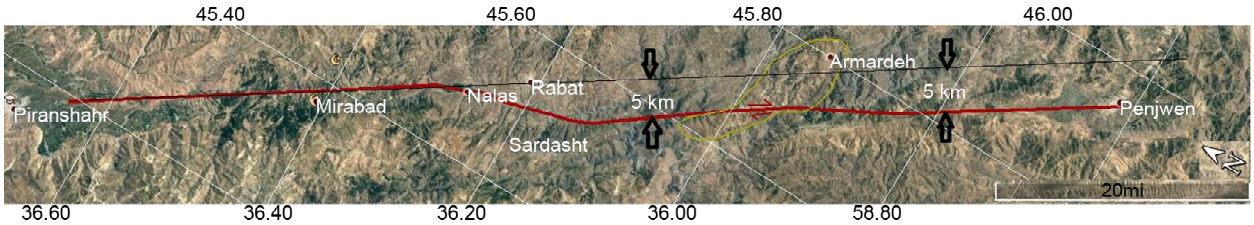

Figure 7. Different conditions of Piranshhar fault before and after the cross point of Armardeh fault.

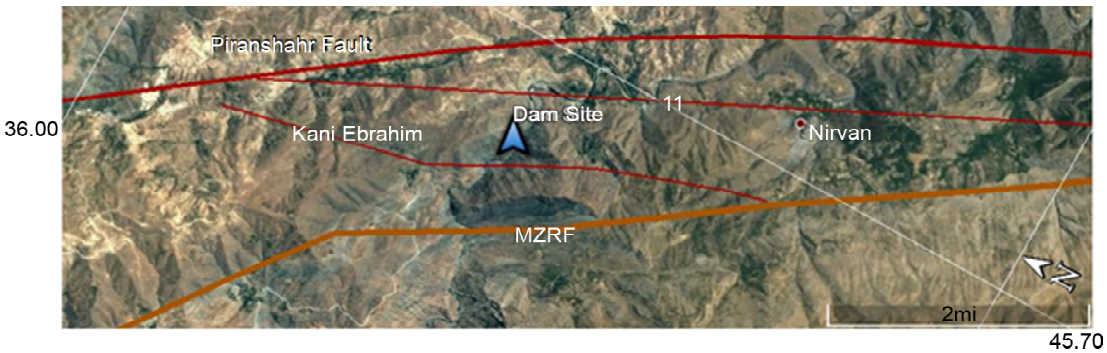

Figure 8. The location of dam site with respect to Piranshahr and other minor faults.

topography (Figure 7).

The Piranshahr fault near the Choman dam site is bended to the northwest, and some minor faults on the inner side of the bend cut the valley and pass from the dam site (F1, F2, Kaniebrahim, and L1 in Figure 8). Kaniebrahim fault, the biggest and most important minor faults, is a thrust fault with a length of 7.5 km, dip to the Northwest, without any sign of recent activity. The L1 lineament originates from the main fault in the south of Kaniebrahim village, passes from about 600 meters south of the site, and continue to the east up to Nirvan village. No outcrop or recent activity of this lineament was observed in field studies. Armardeh and Tajan are another active faults in a radius of 20 km of the site (Figure 9).

4. Probability Fault Displacement Hazard Analysis (PFDHA) Methodology:

Fault displacement assessment is classified into two groups of direct and earthquake evaluation approaches [13, 36].

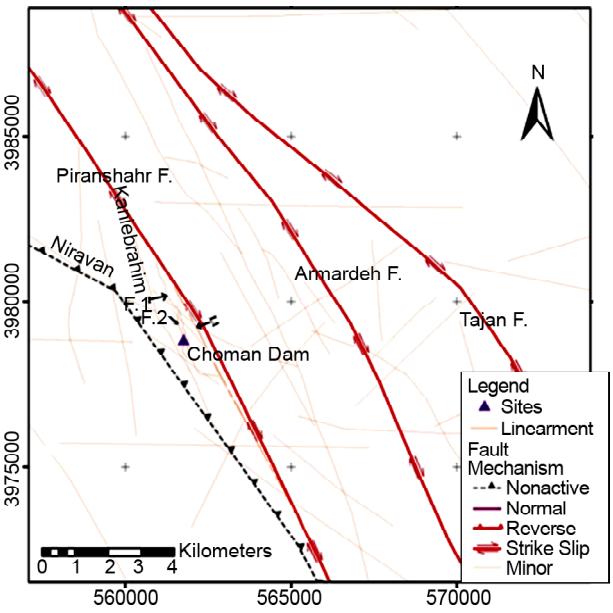

Figure 9. Active faults around the Choman dam site.

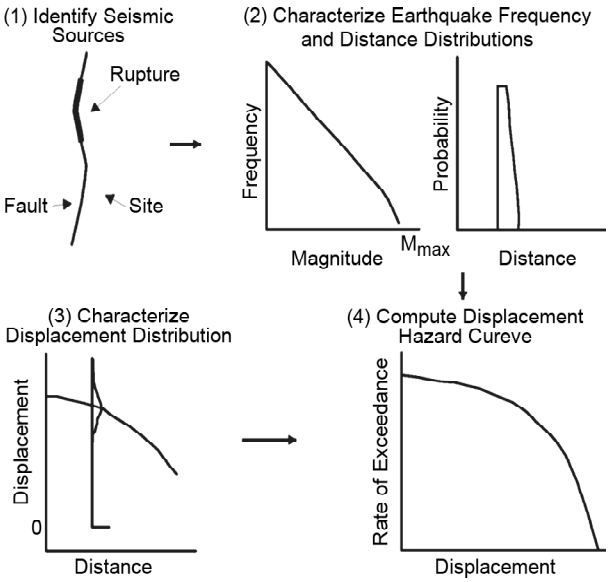

Figure 10. Steps of probability fault displacement hazard study [13].

4.1. Direct Approach

In this method, the probability of slip can be estimated based on the rate of fault displacement and slip distribution function. The frequency of displacement exceedance $\partial(d)$ is given as:

$$\partial(d) = \lambda_{D.E} . P(D > d \mid Slip) \tag{1}$$

where d= displacement, $\lambda_{D.E}$ = rate of displacement events on the fault, $P(D > d \mid Slip)$ = conditional probability that displacement D, for a given event, exceeds d, given that slip on the feature occurs.

The rate of displacement on the fault is assessed by slip dating of all events, and the conditional probability of exceedance slip $(P(D > d \mid Slip))$ can also be obtained by measuring the amount of slip for many events at the site [13]. The necessary data for this approach comes from paleoseismology studies (e.g., [37-38]), which is time-consuming, costly and only applicable in specific geology situations. Therefore, it is impossible to apply for the majority of engineering projects.

4.2. Earthquake Approach

Earthquake approach is similar as the probability seismic hazard evaluation (Figure 10). The fault displacement is maximum over the fault and decrease by distance r from the fault. The annual probability displacement exceedance $\upsilon(d)$ in distance r of the fault can be written as:

$$\upsilon(d) = \lambda_0 \times P_1 \times P_2 \times P_3 \tag{2}$$

where: λ_0 = Rate of fault activity; P_1 = Probability of surface faulting; P_2 = Probability of surface faulting continuing up to distance r from the main fault, P_3 = Probability of fault displacement exceeding d at distance r.

Moreover, the exceedance rate for fault displacement $V_k(d)$ for site k, at distance r from the main fault, and n earthquake events, is defined as [13]:

$$V_k(d) = \sum_n \alpha_n(m_o) \int_{m_o}^{m^u} f_n(m) \times \left[\int_0^{\infty} f_{kn}(r \mid m) . P_{kn}^{*}(D > d \mid m, r) . dr \right] . dm \tag{3}$$

where: $\alpha_n(m_o)$ = the rate of all earthquakes on source n above a minimum magnitude of engineering significance, m_o; $f_n(m)$ = the probability density of earthquake size between m_0 and a m^u (maximum earthquake that source n can produce); $f_{kn}(r \mid m)$ = the conditional probability density function for distance r from site k to an earthquake of magnitude m occurring on source n; $P_{kn}^{*}(D > d \mid m, r)$ = the near surface displacement attenuation function that is defined with Equation (4):

$$P_{kn}(D > d \mid m, r) = P_{kn}(Slip \mid m, r) . P_{kn}(D > d \mid m, r, Slip) \tag{4}$$

$P_{kn}(Slip|m,r)$ is a conditional displacement in the site *k*, given that an earthquake of *m*, at a distance *r* occurs; and $P_{kn}(D>d|m,r,Slip)$ is the probability of *D* exceeding *d*, given that an earthquake *m*, at distance *r*, with surface faulting occurrance.

4.3. Definition of Probability Functions:

The probability of surface faulting (P_{kn}(*Slip*|*m*, *r* = 0)): This features can be estimated by statistical approaches or empirical relationships. Surface faulting can be observed if the width of fault rupture is greater than seismogenic depth. Length and width of fault can be predicted by empirical relationships for a given magnitude. It adopts that the ratio of length to width for normal and reverse faults to be 1, and for strike-slip to be 2. Therefore, it is possible to estimate the probability of surface faulting using a seismogenic depth and width of faulting. The surface faulting probability can also be estimated by empirical relationships that are proposed for all kind of faults [39-41]. Figure (11) shows the surface faulting probability-magnitude curves proposed by Wells and Coppersmith [39], based on the world-wide data (Equation 5).

$$P(slip \mid m, r=0) = \frac{e^{-12.51+2.053M}}{1+e^{-12.51+2.053}} \quad (5)$$

Conditional Probability of Displacement $P_{kn}^{*}(D>d|m,r)$: The conditional probability of displacement, represents the probability that displacement (*D*) in point *k* for a given magnitude *m* and distance *r* exceeds *d*. In fact, this function is like an attenuation relationship in Probablistic Seismic Hazarad Analysis (PSHA) method. The past earthquakes demonstrate that the maximum fault displacement are usually happen in the middle of the fault and decrease to the ends. In an elliptical model, it is supposed that the displacement reached to zero at the end of fault (Figure 12). It has also been found that the ultimate displacement depends on fault type and increases from reverse to the normal and strike-slip faults.

A few conditional probability displacement relationships is available for estimation of fault displacement values [13, 14, 43]. Table (1) and Figure (13) represent different models proposed by Peterson et al. [14] for strike-slip faults, based on the model and parameters defined in Figure (14).

In a case of distributed fault displacement model, it is possible to have a movement at distance '*r*' of the fault. The probability of such displacement became higher with increasing the site dimensions (Z). Peterson et al. [14] introduced the experimental probability functions for estimation of fault displacement probability at distance *r* for different dimensions of *Z* (Table 2).

Probability of Magnitude (f_m (*m*) *dm*): Such

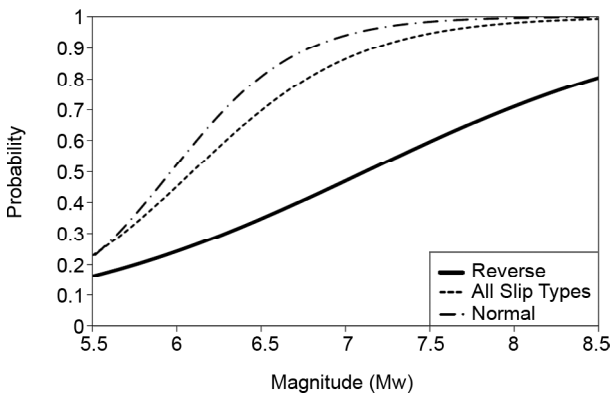

Figure 11. Probability of faulting respect of Magnitude for all kind of fault based on Equation (5) [42].

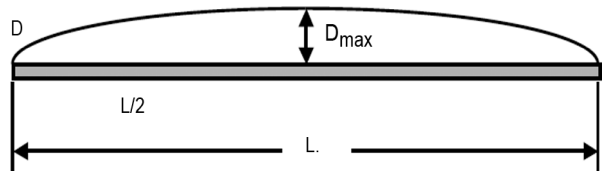

Figure 12. Elliptical model's of displacement distribution [13].

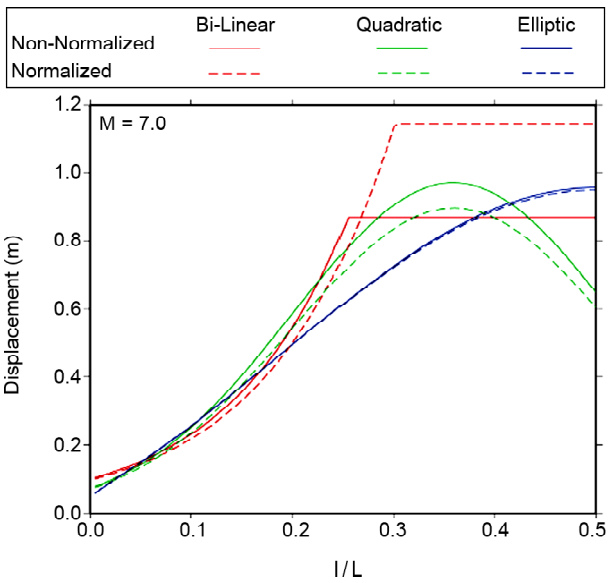

Figure 13. Different slip distribution models of Bilinear, Quadratic, and Elliptic for a magnitude 7, Normalization can be done as displacement divided by maximum or average values [14].

Table 1. Experimental relationship of displacement along the fault [14].

Type of Rapture	Condition	Model	Relationship
Dispalcement Along the Main Fault (D)	Multi Variate	Bilinear	$\ln(D) = 1.7969M_W + 8.5206\left(\frac{l}{L}\right) - 10.2855 \quad \sigma_{ln} = 1.2906 \quad \frac{l}{L} < 0.3$ $\ln(D) = 1.7658M_W + 7.8962 \quad \sigma_{ln} = 0.9624 \quad \frac{l}{L} \geq 0.3$
		Quadarantic	$\ln(D) = 1.7895M_W + 14.4696\left(\frac{l}{L}\right) - 20.1723\left(\frac{l}{L}\right)^2 - 10.54512 \quad \sigma_{ln} = 1.1346$
		Elliptic	$\ln(D) = 3.3041\sqrt{1 - \frac{1}{0.5^2}\left[\left(\frac{l}{L}\right) - 0.5\right]^2} + 1.7927M_W - 11.2192 \quad \sigma_{ln} = 1.1348$
	Normal	Bilinear	$\ln\left(D/D_{avg}\right) = 8.2525\left(\frac{l}{L}\right) - 2.3010 \quad \sigma_{ln} = 1.2962 \quad \frac{l}{L} < 0.3008$ $\ln\left(D/D_{avg}\right) = 0.1816 \quad \sigma_{ln} = 1.0013 \quad \frac{l}{L} \geq 0.3008$
		Quadarantic	$\ln\left(D/D_{avg}\right) = 14.2824\left(\frac{l}{L}\right) - 19.8833\left(\frac{l}{L}\right)^2 - 2.6279 \quad \sigma_{ln} = 1.1419$
		Elliptic	$\ln\left(D/D_{avg}\right) = 3.2699\sqrt{1 - \frac{1}{0.5^2}\left[\left(\frac{l}{L}\right) - 0.5\right]^2} - 3.2749 \quad \sigma_{ln} = 1.1419$
Distributed Faulting Assume (d)	Miulti Variate	Power	$\ln(d) = 1.4016M_W - 0.1671\ln(r) - 6.7991 \quad \sigma_{ln} = 1.1193$
	Normal	Power	$\ln\left(d/D_{avg}\right) = -0.1826\ln(r) - 1.5471 \quad \sigma_{ln} = 1.1388$

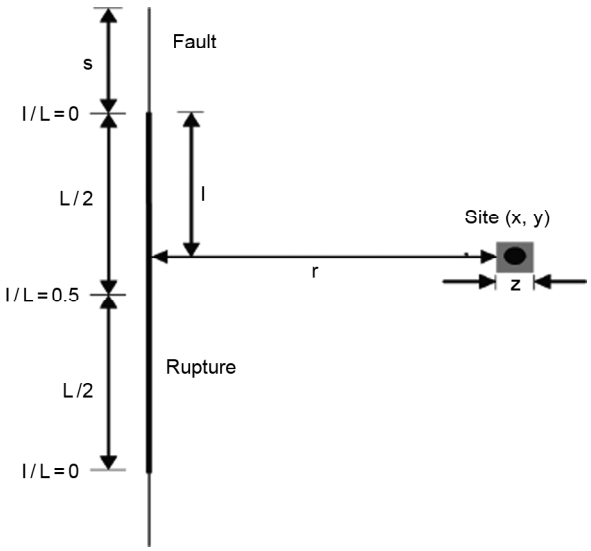

Figure 14. Variables used by Peterson et al. [14].

as in the PSHA, the following function can be used:

$$f_m(m) = \left(\frac{b\ln(10)10^{-b(m-m_o)}}{1-10^{-b(m^u-m_o)}}\right) \quad (6)$$

where b is the slope of Gutenberg-Richter function, mo is a minimum magnitude of interest in earthquake engineering, assumed as 4.0 in this study, and m^u is the maximum magnitude expected or experienced. The m^u is estimated based on the experimental relationship or the historical seismicity of the fault.

Table 2. Different fault displacement probability functions at distance r and Dimension Z [14].

Site Dimension	Fault Displacement Probability Functions
25*25	$\ln(P) = -1.1470\ln(r) + 2.1046 \quad \sigma_{ln} = 1.2508$
50*50	$\ln(P) = -0.9000\ln(r) + 0.9866 \quad \sigma_{ln} = 1.1470$
100*100	$\ln(P) = -1.0114\ln(r) + 2.5572 \quad \sigma_{ln} = 1.0917$
150*150	$\ln(P) = -1.0934\ln(r) + 3.5526 \quad \sigma_{ln} = 1.0188$
200*200	$\ln(P) = -1.1538\ln(r) + 4.2342 \quad \sigma_{ln} = 1.0177$

5. Displacement Hazard Curve of Choman Dam Site

Table (3) shows the characteristics of active faults around the Choman dam site [44]. The maximum magnitude of the fault reported in Table (3) is estimated from the empirical relationship of Wells and Cooperesmith [45] for strike-slip fault. The regional earthquake parameters (β and $\lambda m_o = 4.0$) of the fault are estimated using Kijko and Sellevall [46] for a radius of 150 km from the site. The regional value of β given to all faults and λm_o of each fault is calculated by normalization of regional λm_o using Equation (11):

$$\lambda_{mo}(Fi) = \frac{Li}{L}(\lambda_{mo}(area)) \quad (7)$$

Figures (15) and (16) have shown the magnitude-probability of surface rupture and magnitude-

Table 3. Charachterstics of active fault around the site of Choman [44].

Fault Name		Length (km)	Maximum Magnitude (Mw)	β	$\lambda_{4.0}$	Minimum Distance from the Dam Site (km)
Piranshahr	Main Fault	150	7.3	2.72	0.2716	1.2
						0.6
	Panjvein-Sardasht f.	71	6.9			1.2
						0.6
Armordeh		71	6.9	2.72	0.038	6.8
Tazan		21	6.3	2.72	0.052	4.4

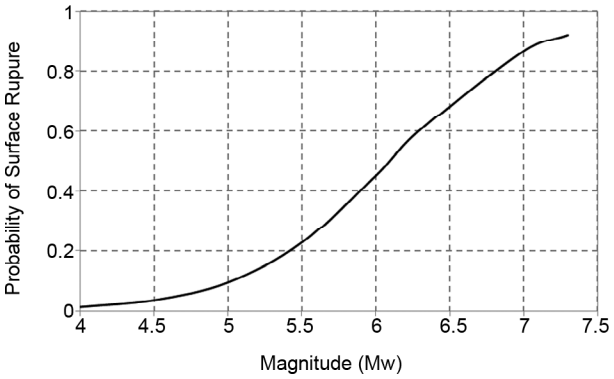

Figure 15. The probability of surface rupture-magnitude curve.

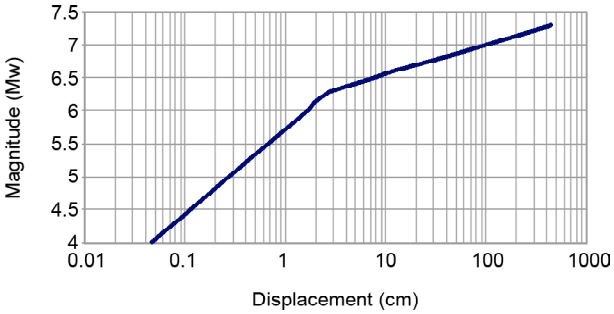

Figure 16. Magnitude-Displacement curve [47].

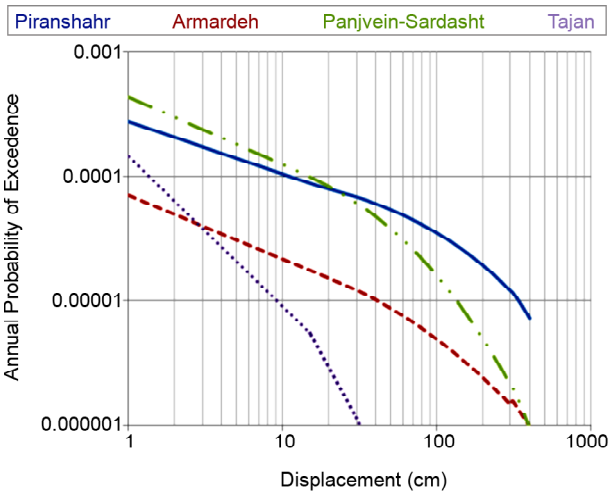

Figure 17. Displacement hazard curve along the fault in the nearest location to the site.

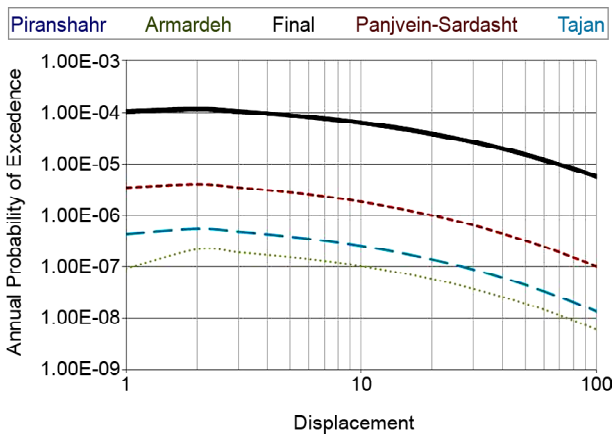

Figure 18. Displacement hazard curve in the site location.

displacement curves based on the Equation (5) and Wells and Cooperesmith [39] relationship. Besides, Figure (17) has shown the displacement hazard curve for all active faults around the site. It is evident that the higher displacement is related to the Piranshahr and Panjvein-Sardasht faults. Figure (18) has demonstrated the annual probability of exceedance of displacement in the dam site for $Z = 150 \times 150$. The Piranshahr hazard curve in Figure (18) is a combination of two curves of Piranshhar and Panjvein-Sardasht segments for two cases of 1200 and 600 meters distance from the dam. The average, upper and lower limits of final displacement hazard curve are demonstrated in Figure (19).

5. Discussion

International Committee of Large Dam (ICOLD) has proposed the different seismic design levels of (i) Maximum Credible Earthquake (MCE), (ii) Safety Evaluation Earthquake (SEE), (iii) Maximum Design Earthquake (MDE), (iv) Design Basis Earthquake (DBE), (v) Operating Basis Earthquake (OBE), and (vi) Construction Earthquake (CE) to seismic design of Large Dams. In Probabilistic Seismic Hazard Evaluation method (PSHA) by assuming a lifetime of 100 years, return periods of 10000, 1000, 475, 145, and 50 years are usually

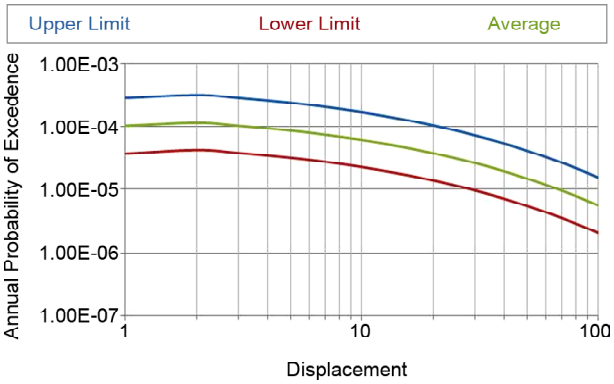

Figure 19. Final displacement hazard curve (average, upper and lower limit).

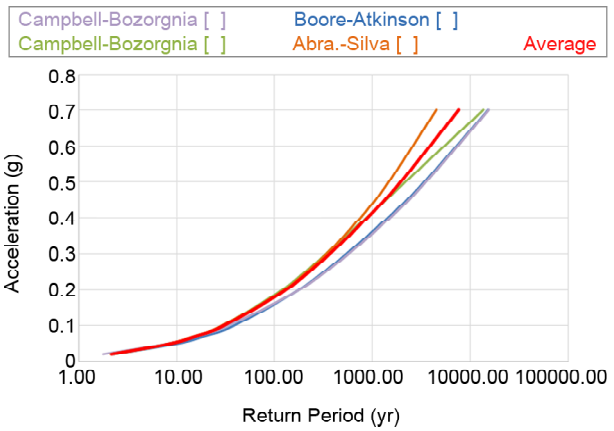

Figure 20. Horizontal Acceleration hazard curve for Choman dam [44].

assigned for estimations of ground shaking parameters in different levels of SEE, MDE, DBE, OBE, and CE, respectively [12]. Figure (20) has shown the horizontal acceleration hazard curve of Choman dam produced by PSHA approach [44]. Comparison of Figures (19) and (20) indicate that the return period of fault displacement is much longer than for acceleration because the fault displacement can only occur in special conditions during the large earthquakes. Therefore, it is believed that the return period for estimation of fault displacement must be much longer than acceleration. Active fault is usually defined as a fault having ruptured within the last 10000-35000 years [48, 50]. In this study, return periods of 10000 and 35000 years are proposed for evaluation of fault displacement in DBE and MDE levels based on the avarage curve and return period of 35000 years; however, upper limit curve is assinged for MCE or SEE design level. Table (4) demonstrated the maximum fault displacement for different return periods based on Figure (19). Therefore, the fault displacement of 20, 30, and 65 cm can be assigned for the seismic design level of DBE, MDE and SEE or MCE, respectively.

Table 4. Avevrage and maximum fault displacement based on Figure (19).

Design Level	Return Period (Years)	Displacement (cm)
DBE	10000	20
MDE	35000	30 (Average Fault Displacement Curve)
SEE/MCE	35000	65 (Maximum Fault Displacement Curve)

6. Conclusion

In this study, the new approach of PFDHA is applied to evaluation of fault displacement at Choman dam site in the west of Iran using the Perterson et al. [14] approach. One of the crucial issues in PFDHA approach is the selection of the return period values of fault displacement. Recent studies emphasized that the criteria of PSHA are unsuitable for PFDHA, and return period for fault displacement must be much longer than PSHA, but no clear criteria has been provided up to now. In this study, based on the definition of an active fault, return periods of 10000 and 35000 years are selected to evaluate the fault displacement for different seismic design. By this, the fault displacement of the site under study for DBE, MDE, and SEE or MCE levels are 20 and 30 and 65 cm, respectively.

References

1. Sherard, J.L., Cluff, L.S., and Allen, C.R. (1974) Potentially active faults in dam foundations. *Geotechnique*, **24**, 367-428.

2. ICOLD (1998) *Neotectonics and Dams Active Faults in Dam Foundation Hazard, Bulletin 112*. Committee on Seismic Aspects of Dam Design, International Commission on Large Dams, Paris.

3. Mejia, L., Walker, J., and Gillon, M. (2005) Seismic evaluation of dam on active surface fault. *Waterpower XIV, Technical Papers CD-Rom, HCI Publications, Kansas City, MO.*, USA.

4. Gillon, M., Mejia, L., Freeman, S.T., and Berryman, K. (1997) Design criteria for fault rupture at the Matahina Dam, New Zealand.

International Journal on Hydropower and Dams, **4**(2).

5. McMorran, T. and Berryman, K. (2001) Late Quaternary faulting beneath Matahina Dam. *Proc. Symp. on Engineering and Development in Hazardous Terrain*, Christchurch, New Zealand Geotechnical Society, 185-193.

6. Allen, C.R. and Cluff, L.S. (2000) Active faults in dam foundations: an update. *Proc. 12th World Conf. on Earthquake Engineering*, Auckland, New Zealand, Paper 2490, 8p.

7. ICOLD (1989) *Selecting Seismic Parameters for Large Dams, Guidelines, Bulletin 72*. Committee on Seismic Aspects of Dam Design, International Commission on Large Dams, Paris.

8. Kerr, J., Nathan, S., Van Dissen, R., Webb, P., Brunsdon, D., and King, A. (2004) *Planning for Development of Land on or Close to Active Faults: A Guideline to Assist Resource Management Planners in New Zealan*d. Published by the Ministry of the Environment, ME Numbers 483 & 565.

9. Bray, J.D. (2001) Developing mitigation measures for the hazards associated with earthquake surface fault rupture. *Proceedings of A Workshop on Seismic Fault-Induced Failures - Possible Remedies for Damage to Urban Facilities*, Japan Society for the Promotion of Science, Tokyo, Japan, 55-79.

10. Bray, J.D. (2009a) Earthquake surface rupture design considerations. *Proceedings of 6th International Conference on Urban Earthquake Engineering*, Tokyo Institute of Technology, Tokyo, Japan, 37-45.

11. Bray, J.D. (2009b) Designing buildings to accommodate earthquake surface fault rupture. *Proceedings of ATC and SEI Conference on Improving the Seismic Performance of Existing Buildings and Other Structures*, San Francisco, USA, 1269-1280.

12. ICOLD (2010) *Selecting Seismic Parameters for Large Dams*. Guidelines, Revision of Bulletin 72. Committee on Seismic Aspects of Dam Design, International Commission on Large Dams, Paris.

13. Youngs, R.R., W.J. Arabasz, R.E., Anderson, A.R., Remelli, J.P., Ake, D.B., Slemmons, J., McCalpin, D.I., Doser, C.J., Fridrich, F.H., Swan, A.M., Rogers, J.C., Yount, L.W., Anderson, K.D., Smith, R., Bruhn, P.L.K., Knuepfer, R.B., Smith, C.M. dePolo, D.W., O'Leary, K.J., Coppersmith, S., Pezzopane, D.P., Schwartz, J.W., Whitney, S.S., Olig, and G.R., Toro (2003) Probabilistic fault displacement hazard analysis PFDHA. *Earthquake Spectra*, **19**(1), 191-219.

14. Petersen, M.D., Timothy, E.D., Chen, R., Cao, T., Wills, C.J., Schwartz, D.P., and Frankel, A.D. (2011) Fault displacement hazard for strike-slip faults. *Bulletin of the Seismological Society of America*, **1012**, 805-825.

15. Moss, R.E.S. and Ross, Z.E. (2011) Probabilistic fault displacement analysis for reverse faults. *Bulletin of the Seismological Society of America*, **101**(4), 1542-1553.

16. Wells, D.L. and Kulkarni, V.S.,(2014) Probabilistic and deterministic fault displacement hazard analysis – sensitivity analyses and recommended practices for developing design fault displacements. *Proceedings of the 10 the National Conference on Earthquake Engineering*, Earthquake Engineering Research Institute, Anchorage, AK

17. Robb Eric S. Moss and Zachary E. Ross (2011) Probabilistic fault displacement hazard analysis for reverse fault. *Bulletin of the Seismological Society of America*, **101**(4), 1542-1553.

18. Hart, E.W. (1996) *Pisgah, Bullion and Related Faults*. California Division of Mines and Geology Fault Evaluation, Report FER-188, 1987. Mccalpin, J. Paleoseismology-San Diego, Acad. Press, 588p.

19. Bonilla, M. (1970) Surface faulting and related effects. *Earthquake Engineering. Prentice-Hall, Seismol. Soc. Am.*, **84**, 974.

20. Fenton, CH. and Dober, MC. (2000) Characteristics of the surface rupture associated with the 16 October 1999 Hector Mine, California

earthquake. *Seismological Research Letters*, **71**(2), 223.

21. Bray, JD., Seed, RB., Cluff, LS., and Seed, HB. (1994) Earthquake fault rupture propagation through soil. *ASCE Journal of Geotechnical Engineering*, **1203**, 453-561.

22. Treiman, J.A. (2009) Surface faulting and deformation assessment and mitigation. *PEER Workshop on Surface Fault Displacement Hazard.*

23. Bernard, X.D., Labaume, P., Darcel, C., Davy, P., and Bour, O. (2002) Cataclastic slip band distribution in normal fault damage zones, Nubian sandstones, Suez Rift. *Journal of Geophysical Research*, **107**(B7), 2141, 10.1029/2001JB000493.

24. Tchalenko, J.S. and Braud, J. (1974) Seismicity and structure of the Zagros: the main recent fault between 33° and 35°N. *Phil. Trans. R. Geol. Soc. Lond.*, **277**, 1-25.

25. Motaghi, K., Shabanian, E., and Kalvandi, F. (2017) Underplating along the northern portion of the Zagros suture zone, Iran. *Geophysical Journal International*, **210**(1), 375-389.

26. Gidon, M., Berthier, F., Billiaut, JP., Halbronn, B., and Maurizot, P. (1974) Sur les caractères et l'ampleur du coulissement de la "Main Fault" dans la région de Borudjerd-Dorud Zagros oriental, Iran. *Cr. Acad. Sci.*, **278**, 701-704 (in French).

27. Talebian, M. and Jackson, J. (2002) Offset on the Main Recent Fault of NW Iran and implications for the late Cenozoic tectonics of the Arabia-Eurasia collision zone. *Geophys. J. Int.*, **150**, 422-439.

28. Walpersdorf, A., Hatzfeld, D., Nankali H., Tavakoli, F., Nilforoushan, F., Tatar, M., Vernant, P., Chéry, J., and Masson, F. (2006) Difference in the GPS deformation pattern of North and Central Zagros (Iran). *Geophysical Journal International*,**167**(3), 1077-1088

29. Khodaverdian, A., Zafarani, H., and Rahimian, M. (2015) Long term fault slip rates, distributed deformation rates and forecast of seismicity in the Iranian plateau. *Tectonics*, **34**(10), 2190-2220.

30. Vernant, P., Nilforoushan, F., and Hatzfeld, D. (2004) Present-day crustal deformation and plate kinematics in the Middle East constrained by GPS measurements in Iran and northern Oman. *Geophysical Journal International*, **157**, 381-398.

31. Eftekhar-Nezhad, J. (1972) *Geological Map Kashmar, 1:250,000.* Geol. Surv. of Iran, Tehran (in Press).

32. Bachmanov, D.M., Trifonov, V.G., Hessami, K.T., Kozhurin, A.I., Ivanova, T.P., Rogozhin, E.A., Hademi, M.C., and Jamali, F.H. (2004) Active faults in the Zagros and central Iran. *Tectonophysics*, **380**, 221-241.

33. Mohajjel, M. and Rasouli, A. (2014) *Structural Evidence for Superposition of Transtension on Transpression in the Zagros Collision Zone: Main Recent Fault, Piranshahr Area, NW Iran.*

34. Ambraseys, N.N. and Melville, C.P. (1982) *A History of Persian Earthquakes.* Cambridge University Press, 219p.

35. Berberian, M. (1995) Master blind thrust faults hidden under the Zagros folds active basement tectonics and surface morphotectonics. *Tectonophysics*, **241**, 193-224.

36. Hofmann, R. (1991) *Probabilistic Fault Displacement and Seismic Hazard Analysis Literature Assessment.* CNWRA 91-013, 1-146.

37. McCalpin, J.P. (1996) *Paleoseismology.* Academic Press, San Diego, 588 p.

38. Wallace, R.E. (1981) 'Active faults, paleoseismology, and earthquake hazards in the western United States'. In: Earthquake Prediction: An International Review. D.W. Simpson and T.G. Richards, eds., Maurice Ewing Ser. 4.

39. Wells, D.L. and Coppersmith, K.J. (1993) Likelihood of surface rupture as a function of magnitude abs. *Seismological Research Letters*, **64**(1), 54p.

40. DePolo, C.M. (1994) The maximum background earthquake in the basin and range. *Bulletin of*

the Seismological Society of America, **84**, 466-472.

41. Pezzopane, S.K. and Dawson, T.E. (1996) *Fault Displacement Hazard: A Summary of Issues and Information, in Seismotectonic Frame work and Characterization of Faulting at Yucca Mountain, Nevada*. U.S. Geological Survey Administrative Report prepared for the U.S. Department of Energy, Chapter 9, 160p.
42. Coppersmith, K.J. and Youngs, R.R. (1992) Modeling fault rupture hazard for the proposed repository at Yucca Mountain, Nevada. *Proceedings of the Third International Conference, High-Level Radioactive Waste Management*, Las Vegas, Nevada, V.I., 1142-1150.
43. Braun, J.B. (2000) *Probabilistic Fault Displacement Hazards of the Wasatch Fault*. Master's Thesis, Department of Geology and Geophysics, University of Utah, Salt Lake City, Utah.
44. Hafezi Moghaddas, N. (2016) *Seismic Hazard Evaluation of Choman Dam Report*. Zamin Physic Poua Co. (in Persian).
45. Wells, D.L. and Coppersmith, K.J. (1994) New empirical relationships among magnitude, rupture length, rupture width, rupture area, and surface displacement. *Bulletin of the Seismological Society of America*, **84**(4), 974-1002.
46. Kijko, A. and Selevoll, M.A. (1992) *Estimation of Earthquake Hazard Parameters from Incomplete Data Files*. Part II. Incorporation of magnitude heterogeneity, 213p. Int. 93.
47. Wells D. and Coppersmith, K. (1993) Likelihood of surface rupture as a function of magnitude abs. *Seismol. Res. Lett.*, **64**(1), p. 54.
48. Fraser, W.A. (2001) California Division of Safety of Dam Fault Activity Guidelines. Available at: http://www.water.c.a.gov/dansafety/docs/fault.pdf. Accessed Dec. 3, 2010. California Department of Water Resources.
49. Slemmons, D.B. and McKinney, R. (1977) *Definition of Active Fault*. U.S. Army Engineer Waterways Experiment station, Miscellaneous Paper S-77-8.
50. Bryant, W.A. and Hart, E.W. (2007) Fault-Rupture Hazard Zones in California-Alquist-Priolo Earthquake Fault Zoning Act with Index to Earthquake Fault Zone Map Zone. *California Geological Survey Special Publication*, 42, 38p., digital version available online at ftp://ftp.consrv.ca.goc.